Response to Referee #3

This study continues the work in Schmedding (2020), implemented three different glass transition temperature Tg parameterization in a newer version of CMAQ that uses parameterized organic hygroscopicity parameter kappa. This manuscript presents new advancement in improving organic aerosol phase state resolving in atmospheric chemistry modeling. However, several issues remain. I recommend major revision before acceptance.

Major Comments:

Aerosol liquid water and water uptake are central to this manuscript. The newer CMAQ can model organic-layer water uptake, which is the main advance over Schmedding (2020). Please expand Results/Discussion to compare directly with Schmedding (2020) using the same Shiraiwa et al. 2017 parameterization and to show how different water uptake schemes affect the results. Also move the statement about no water transfer between core and shell in the phase separation setup earlier in the manuscript.

We thank the reviewer for this recommendation and have made the following changes to our manuscript to address the inclusion of this central science update:

3.2 Impacts of modeling dynamic water uptake to the organic coating on phase state

375 One major advancement in CMAQv5.3 is the addition of hygroscopicity parameters to track the uptake of water to modelled organic species (Appel et al., 2021; Pye et al., 2017). In comparison to Schmedding et al., 2020 we find that this update increases w_s by up to 0.05-0.25 (Fig. S2) over the eastern and northern part of the domain at the surface (layer 1), resulting in decreases in $T_g(w_{org}):T$ by 0.05-0.15 (Fig. S3). The w_s largely decreases over the oceans in this study compared to Schmedding et al., 2020 and can be partially attributed to increased ALW over the oceans (which result in higher w_s in
380 Schmedding et al., 2020; $w_s \geq 0.6$) and relatively lower OA concentrations over the oceans (compared to land) that have resulted in less hygroscopic water uptake ($0.2 \leq w_s \leq 0.6$) to the organic coating in our model runs. Differences in w_s decrease with height given the lack of humidity at higher altitudes (Fig. S2 c-d), however are still higher in Schmedding et al., 2020 resulting in increases in $T_g(w_{org}):T$ in our model runs in comparison (Fig. S3 c-d).

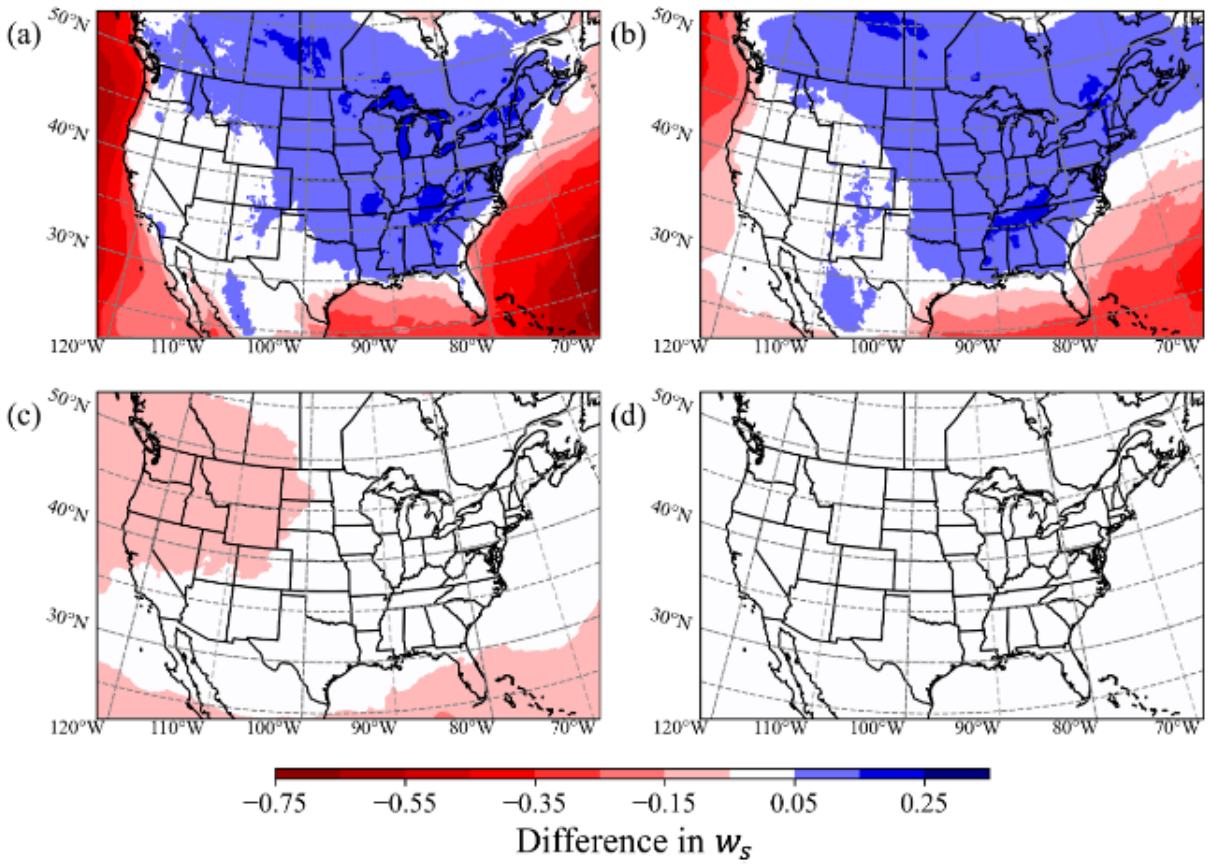

Supplemental Figure 2. Difference in w_s predicted in the study in comparison to those predicted by Schmedding et al., 2020 and in this study for the entirety of the 2013 SOAS Field Campaign (June 1st – July 31st, 2013) for the surface layer; 1-0.9975 atm (a)), layer 18 (corresponding to ~1.8km; 0.82-0.8 atm (b)), layer 28 (corresponding to ~8km; 0.4-0.35 atm (c)), and layer 35 (corresponding to ~17km; 0.05-0 atm (d)). The difference expressed is unitless as w_s is a fraction.

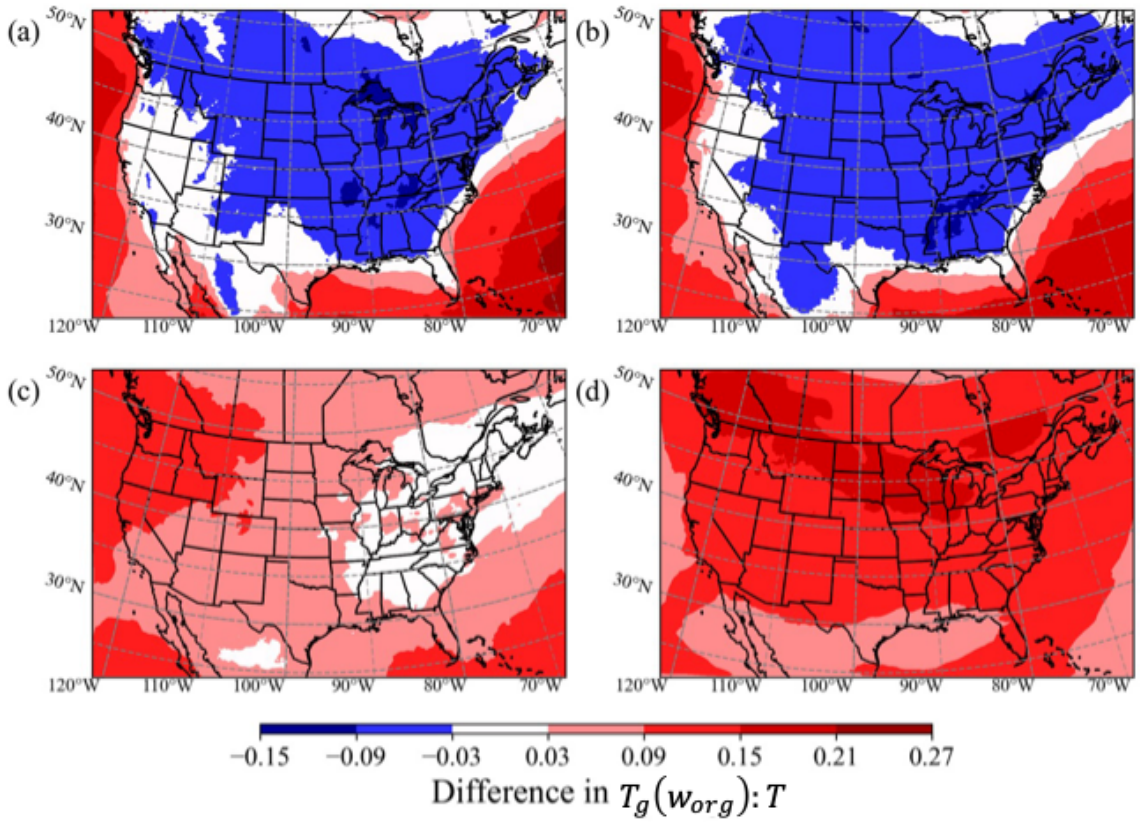

Supplemental Figure 3. Difference in $T_g(w_{org}):T$ predicted in the study in comparison to those predicted by Schmedding et al., 2020 and in this study for the entirety of the 2013 SOAS Field Campaign (June 1st – July 31st, 2013) for the surface layer; 1-0.9975 atm (a)), layer 18 (corresponding to ~1.8km; 0.82-0.8 atm (b)), layer 28 (corresponding to ~8km; 0.4-0.35 atm (c)), and layer 35 (corresponding to ~17km; 0.05-0 atm (d)). The difference expressed is unitless as $T_g(w_{org}):T$ is a fraction.

4 Discussion

4.1 Modulators of organic coating phase state

Model predictions show that both the w_s and the choice in T_g parameterization impact the phase state of the organic coating on phase-separated aerosols. Previous studies have shown the influence of ALW on the phase state of organic aerosols

(DeRieux et al., 2018; Rasool et al., 2021). In comparison to assuming 10% of ALW is in the organic coating, we find in using a w_s that is based on OA chemical properties, that organic coatings are more liquid in comparison to Schmedding et al., 2020 (Fig. S2-3) over the eastern and northern parts of the contiguous U.S. domain and therefore may be less of a diffusional barrier to heterogeneous reactive uptake (Schmedding et al., 2020). The assumption that water uptake to the organic coating as

And then have moved acknowledgement that we do not model water movement between the inorganic core and the organic shell up to the methods:

represent the potential resistance to IEPOX reactive uptake in a phase-separated aerosol particle where l_{org} is the organic coating thickness, H_{org} is the Henry's Law coefficient dictating the dissolution of IEPOX into the organic coating (2×10^6 M atm^{-1}) (Zhang et al., 2018b), $D_{org,eff}$ is the diffusivity of IEPOX through organic coating (Fig 1, Eq. 7), and r_{core} is the radius of the inorganic aqueous core. When there is no phase separation $l_{org} = 0$, cancelling out the third resistor term and $r_{core} = r_p$ thus reverting equation S3 to the original parameterization of IEPOX reactive uptake currently in CMAQ. It is important to note that we do not simulate water movement between the aqueous inorganic core and the organic coating, and therefore are unable to capture the impacts of dilution of acids and nucleophiles involved in IEPOX reactive uptake.

Kappa parameterizes equilibrium water uptake. The manuscript notes that aerosol can become semi-solid or solid at higher altitudes. Please discuss the potential bias from applying the same Kappa and equilibrium water uptake to semi-solid or glassy aerosol, and outline what observations and modeling are needed to represent non-equilibrium water uptake in such phases.

We thank the reviewer for raising this point of discussion and appreciate the opportunity to explore these impacts.

In looking into the potential impacts of phase state on hygroscopic growth, to our knowledge, the impacts of assuming equilibrium water uptake for semi-solid/solid particles are mixed and the relationship between chemical composition and equilibrium water uptake is more consistent.

Parsons et al., 2004 and found that succinic acid and adipic acid deliquesced across temperature ranges of 243K-293K at 100% RH, however malonic acid and glutaric acid deliquesced at lower RH for higher temperatures (Parsons et al., 2004). In Hodas et al., 2015, it was found that the presence of this viscous sucrose decreased efflorescence, and that using thermodynamic modeling approaches assuming different phase states produced varied results for different species, however, did not always show the solid phase state producing more inhibition to hygroscopic growth (Hodas et al., 2015). In Lienhard et al., 2015 it was found that hygroscopic growth impacts can't be isolated to its phase state and also found that measured water diffusion onto glassy aerosols was faster than previously reported (Lienhard et al., 2015). In a recent feature article by Diveky et al., 2021 it was found that for different species there were different trends in water accommodation coefficients with increases in temperatures (some increasing and some decreasing) (Diveky et al., 2021). Lastly, in a recent review article on the impacts of organic aerosols on hygroscopic growth by Tan et al., 2024 – although impacts of phase state on hygroscopic growth were pointed to, articles cited explored the impacts of phase separation on hygroscopic growth (finding thicker coatings – not necessarily more viscous coatings – were the cause of lower growth factors) (Li et al., 2021; Maskey et al., 2014; Tan et al., 2024).

The impacts of organic aerosol composition on hygroscopic growth has been more widely studied, measured, and continues to conceptualize aerosol water accommodation (Jimenez et al., 2009; Lambe et al., 2011; Massoli et al., 2010; Pajunoja et al., 2015; Tan et al., 2024).

We make the following changes to our discussion to note upon this:

heterogeneous reactive uptake (Schmedding et al., 2020). The assumption that water uptake to the organic coating as parameterized ignores the phase state may introduce bias, however, to our knowledge a consistent relationship between organic aerosol phase state and hygroscopic growth has yet to be explored (Diveky et al., 2021; Hodas et al., 2015; Lienhard et al., 2015; Pajunoja et al., 2016; Parsons et al., 2004; Tan et al., 2024), as opposed to the relationship between O:C ratio and hygroscopic growth (Jimenez et al., 2009; Lambe et al., 2011; Massoli et al., 2010; Pajunoja et al., 2015).

Specific Comments:

Line 98: Please use em dash (—) instead of hyphen (-)

We thank the reviewer for the recommendation and have made the following change here and throughout the manuscript

observationally-derived phase state data from the Centreville, Alabama, supersite during the 2013 SOAS campaign, although predicting a less viscous phase state than observed (Schmedding et al., 2020; Zhang et al., 2018a). Recently, starting with CMAQv5.3.2, OA hygroscopicity parameters (κ_{org})—which dictate the amount of water that can be taken up by oxygenated

Line 103–115: Please acknowledge other Tg parameterizations that might not be O:C ratio or volatility based (e.g., Galeazzo and Shiraiwa, 2022, "Predicting glass transition temperature and melting point …"). Explain why they are not included, and justify selecting the three used here.

We chose not to incorporate the Tg parameterization from Galeazzo and Shiraiwa, 2022 for two reasons. The primary reason was that our model simulations were done in 2020-2021, therefore, prior to the publication of this article. While the AI model developed to predict Tg in Galeazzo and Shiraiwa appears to perform well against the data they use to evaluate it with, a lot of assumptions would have to made for its implementation into CMAQ. Many modeled OA species within the SAPRC mechanism (and CB6 mechanism) are lumped and do not have representative SMILES strings. Identifying all structures that contribute to OA mass is an ongoing area of research, however, in the development of a chemical mechanism, species are defined by lumped/assumed molecular weights, oxygen to carbon ratios, and saturation concentrations from chamber experiments. We selected the Shiraiwa et al., 2017, the Zhang et al., 2019, and the Li et al., 2020 Tg parameterizations because they were defined with these OA species properties in mind. We agree, however, that the reasoning in choosing the Tg parameterizations could be clearer and have made the following changes:

105 to be systematically compared.

New relationships between T_g and OA M, $O{:}C$, and saturation concentrations (C^0) – which are properties that commonly define OA species in air quality models -- have recently been derived and are summarized in Table 1 (Li et al., 2020; Zhang et al., 2019b). In Li et al. (2020), a T_g equation was fit using a multi-linear least squares regression with $O{:}C$ and C^0 used as
110 independent variables (Li et al., 2020), which can be applied to the information available with the two-dimensional volatility basis set framework (Donahue et al., 2011). This T_g parameterization expanded the training data in comparison to Shiraiwa et

And

This study aims to explore the impacts of phase separation and phase state of the organic coating on modeled IEPOX heterogeneous reactive uptake, taking advantage of recently published T_g parameterizations that were derived taking into
130 consideration commonly encoded chemical transport model OA properties (M, $O{:}C$, and C^0) (Table 1) (Li et al., 2020; Shiraiwa et al., 2017; Zhang et al., 2019b). The phase state algorithms, previously used to calculate bulk OA phase state, can

Line 159–160: The resistor term for IEPOX uptake is central to later discussion and should be included, at least in part, in the main manuscript. The rate constant kparticle should be introduced here. kparticle was never formally introduced in the main manuscript, but only later discussed on page 18 and page 22. In addition, it is stated in earlier texts that the implementation of phase separation and phase state follow Schmedding (2020), is the IEPOX reactive uptake in this study handled differently?

We have moved text describing IEPOX reactive uptake from the supplement into the main text. The treatment of IEPOX reactive uptake in this study is only handled differently with respect to how phase state is calculated (for different model runs with different Tg parameterizations).

Figure 1: The equations and conditions (red texts) are hard to read in the figure. Since they follow Schmedding (2020), re-define the full equations in the Supplement and reference them in this schematic only. The flowchart should present each step clearly without the full equations. The three different Tg parameterization should be shown in three parallel steps instead of in one step.

We increased the clarity of Figure 1. We do, however, find utility in defining full equations and conditionals in this figure as a quick reference for readers. There are different steps within the phase separation and phase state algorithm with conditionals that, spelt out in paragraph form, may cause visual fatigue that we aim to avoid. The three different Tg parameterizations are shown in one step with the specification of either/or because for each model run this algorithm is followed using just one of these equations. Having them illustrated in parallel in this figure may cause confusion and lead the reader to think that all are being calculated in parallel in one model run. We do make the following changes to this section to clarify:

2.3 Implementation of phase separation and phase state

A summary of the CMAQ algorithm used for determining phase separation and phase state are shown in Figure 1, mirroring the implementation of the "PhaseSep2" model setup documented in (Schmedding et al., 2020), with the exception of using individual T_g from multiple studies (Li et al., 2020; Shiraiwa et al., 2017; Zhang et al., 2019b). As shown in Fig. 1, phase separation was determined based on the separation relative humidity (SRH) and occurs when the SRH ≥ RH (Bertram et al.,

2011; You et al., 2014). The SRH was determined based on aggregated aerosol $O:C$ ($O:C_{avg}$) and organic matter to inorganic sulfate ratios ($OM:IN_{sulf}$) (Bertram et al., 2011; Schmedding et al., 2020; Song et al., 2018; Zuend et al., 2012). The $O:C$ were derived from organic matter-to-organic carbon ratio ($OM:OC$) using the relationship published in Simon and Bhave (Simon et al., 2012). If phase separated, either the Shiraiwa, Zhang, or Li T_g equations (explained in section 2.4) are used to calculate the T_g of individual OA species. The individual T_gs are aggregated by source type (anthropogenic or biogenic) and then Eq. 2 (shown in Fig. 1) is used to calculate the overall T_g of the organic coating accounting for water, referred to from here-on-out as $T_g(w_{org})$. The $T_g(w_{org})$:T ratios were then used determine the viscosity of the organic coating (η_{org}) (Eq. 3-6 shown in Fig. 1) using a modified Vogel-Tamman-Fulcher equation (Angell, 1991; DeRieux et al., 2018; Fulcher, 1925; Schmedding et al., 2020; Tammann et al., 1926; Vogel, 1921). Equations for the viscosity of the aerosol (i.e., Eq. 3-6) and ultimately the diffusivity of IEPOX through the organic coating ($D_{org,eff}$, Eq. 7) are also provided in Fig. 1.

And also spell out the Shiraiwa equation in section 2.4

2.43 CMAQ Implementation of Glass Transition Temperature

The details ~~of the implementation~~ of the Shiraiwa et al. (2017) T_g equation and it's formulation ~~parameterization~~ is provided in Schmedding et al., 2020 and Shiraiwa et al., 2017 (Schmedding et al., 2020; Shiraiwa et al., 2017):

285

$$T_{g,i,S} = -21.57 + 1.51M - 0.0017M^2 + 131.4(O:C) - 0.25M(O:C) \quad (15)$$

The details ~~for the implementation~~ of the Zhang et al. (2019b) and Li et al. (2020) T_g equation and their formulation ~~parameterizations~~ are provided below.

Line 168–172 is unclear and requires clarification. I also don't see why the case ws = 0 needs special treatment, as the Gordon-Taylor equation (eq.2) is fine when one component's (in this case water) mixing ratio is 0. Additionally, please use em dash (—) instead of hyphen (-) for in sentence explanatory phrases. What does it mean by switch equations?

We have made the following changes to clarify:

When $w_s = 0$, the aggregated OA phase state equation (Eq. 82) collapses into ~~is equal to~~ the mass fraction weighted aggregated ~~T_gs, previously referred to as the~~ dry phase state equation, represented by $T_{g,org}$ (Dette et al., 2014; Li et al., 2021; Li et al., 2020):

$$T_{g,org} = w_a T_{g,a} + w_b T_{g,b} \quad (14)$$

~~.~~ Given there ~~numerical precision of CMAQ and the likelihood of very small w_s values characteristic of dry OAs yet still greater than zero~~ was never an occurrence during our modeling where ~~the occurrence of~~ $w_s = 0$ ~~was minimal~~, we ~~. A recent~~

~~publication~~ use ~~defined the~~ equation 14 when ~~dry phase state as~~ $w_s \leq 0.1$ (Rasool et al., 2021), signifying a dry aggregate glass transition temperature that does not consider water uptake to the organic shell. While our implementation of phase separation and phase state in CMAQ did~~does~~ not implement in-model conditionals to switch between using $T_g(w_{org})$ and $T_{g,org}$ ~~phase state equations~~ based off of these w_s thresholds~~values~~, we identify dry aerosol phase state instances offline ~~using this threshold and refer to it as $T_{g,org}$~~.

Figure 3 is ineligible. It looks like it is related to the conversion during manuscript upload. Please re-upload the figure in the rebuttal.

We have re-uploaded this figure with some changes suggested by other reviewers:

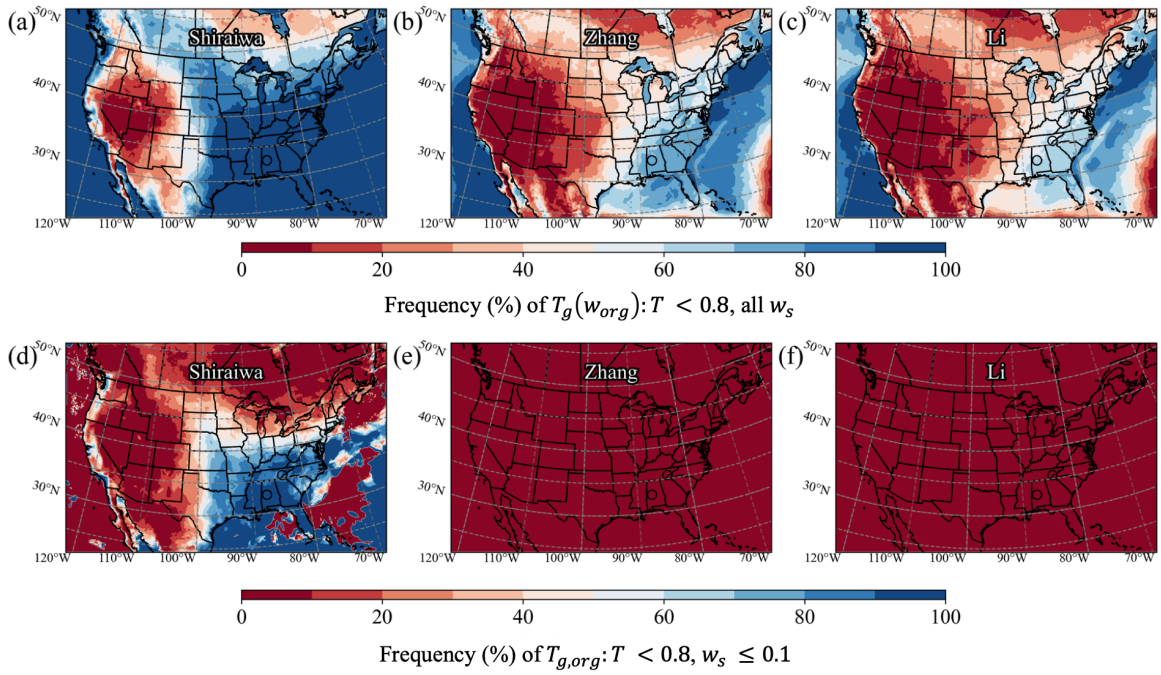

Figure 3. Frequency that the organic coating is in the liquid phase state during the SOAS 2013 Field Campaign episode (June 1st – July 15th, 2013) for the (a & d) Shiraiwa, (b & e) Zhang and (c & f) Li parameterizations for all ~~when~~ w_s ~~> 0.1~~ in the organic coating (a-c) and when $w_s \leq 0.1$ in the organic coating (d-f) across hourly model estimates. Black open circles in each panel correspond to Look Rock, Tennessee (LRK) and Centreville, Alabama (CTR) SOAS observation sites.

Table 2. Species description is ineligible. For the Tg comparison, a three-panel scatter plot (one scheme to scheme comparison in each panel) would be better, with points color coded by O:C or volatility, a 1:1 line, and RMSE in each panel.

We thank the reviewer for their suggestion and realize the utility of one of these plots in contextualizing our results and thus have created the suggested scatter plot to put in the Supplement:

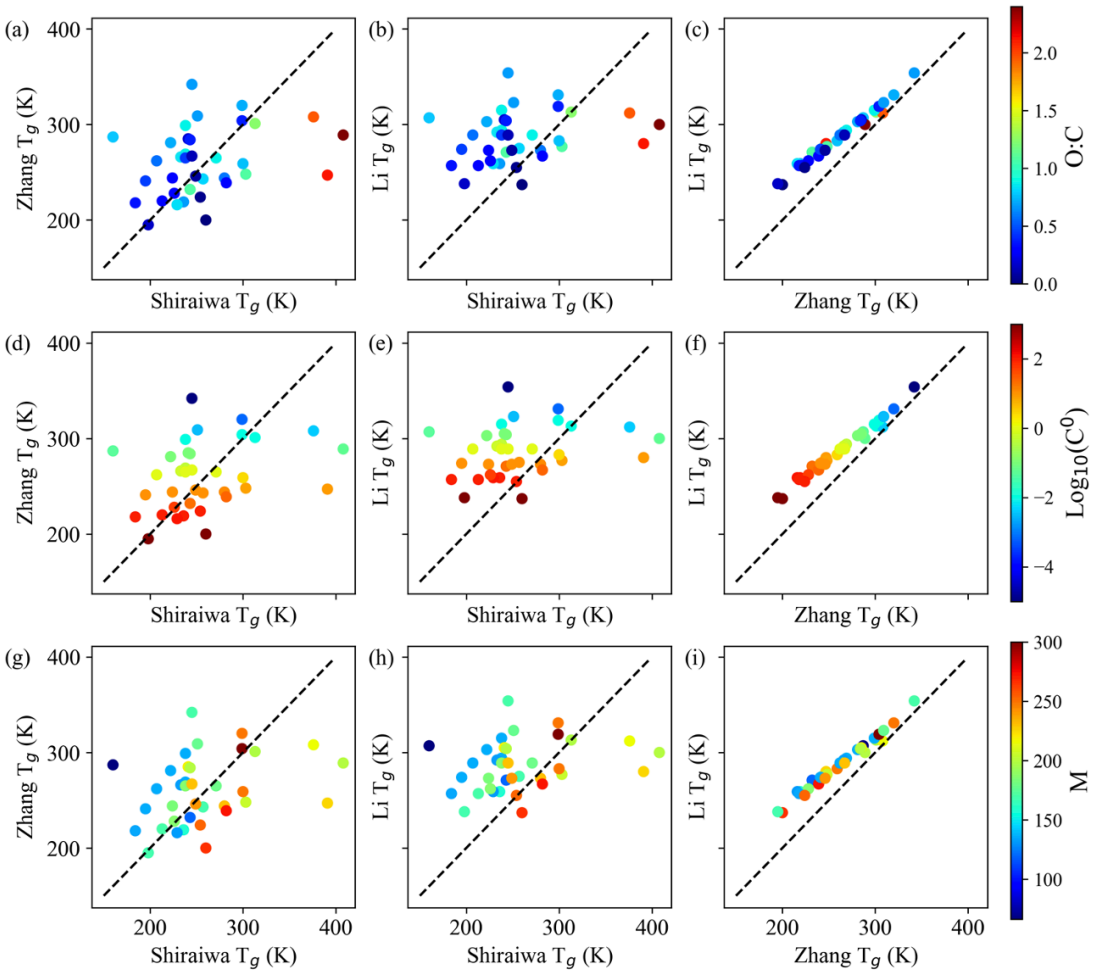

Supplemental Figure 4. Comparison of T_g between the Shiraiwa and Zhang equations (a, d, and g) the Shiraiwa and Li equations (b, e, and h) and the Zhang and Li equations (c, f, and j) colored by O:C (a-c), volatility (d-f) and molecular weight (g-j)

And have added the following explanatory text in the main manuscript:

For most species, the Zhang and Li equations predict a higher T_g than the Shiraiwa equation, and the Li equation predicts a higher T_g than the Zhang equation (Fig. S4). There are some exceptions to this trend where the Shiraiwa Tg equation predicts

a higher Tg than both Zhang and Li for AISOPNN, methacrolein epoxide derived organosulfate (AIMOS), and AIEOS (Table 2), due to their higher O:C (Table 2, Fig. S4 a-b). The relationship between the Zhang and Li T_g predictions are linear (Fig. S4 c, f, and i) in agreement with findings in Li et al., 2020~~,~~ with higher volatility species having a higher T_g predicted by Li in comparison to that predicted by Zhang (Fig. S4 f) (Li et al., 2020). Two CMAQ species of note that have a much higher predicted T_g by Zhang and Li than by Shiraiwa are ~~particularly~~ potential combustion SOA (APCSO) and glyoxal- and methylglyoxal-derived aerosol (AGLY). The M of APCSO is 170 g/mol and the $O:C$ is 0.67, however it has the lowest C^0 of

We were not able to calculate an RMSE as we would have to make an assumption that one set of Tg predictions were the truth/observed and didn't feel that was appropriate.

In this paper we aim to point out areas where air quality models require improvement/attention if they want to implement organic aerosol phase state. We walk through species of importance (given their mass abundance) and their difference in Tg across different equations in what was section 3.3 (now section 3.4) so that future work can better constrain Tg for those species. The utility of the table is a clear illustration of Tg differences on a species-by-species level (which one is not able to convey with a scatter plot where scatters are label-less). We choose to leave this table in the main text, however, agree that the species descriptions were too small and so removed that column and refer readers to the full species properties table in the Supplement:

CMAQ Species	Molar Mass (g mol^{-1})	$\log_{10}(C^0)$	O:C	Source	Shiraiwa T_g (K)	Differences (K) (Zhang @298K - Shiraiwa)	Differences (K) (Li - Shiraiwa)	Differences (K) (Li - Zhang @298K)
AISOPNN	226	0.94	2.11	biog	391	-143	-111	33
AIMOS	200	-1.25	2.40	biog	408	-119	-108	11
AIEOS	216	-2.40	1.95	biog	376	-68	-64	4
AIVPO1	266	3.00	0.00	anth	260	-60	-23	37
AOLGA	206	0.88	1.07	anth	303	-55	-25	30
ASQT	273	1.40	0.28	biog	282	-43	-15	28
AOLGB	248	0.42	0.75	biog	300	-41	-17	24
AMTNO3	231	1.08	0.59	biog	280	-35	-7	29
ASVPO3	253	2.00	0.03	anth	254	-30	1	31
AAVB4	158	2.00	0.67	anth	236	-16	23	40
AAVB3	169	1.00	0.81	anth	257	-14	18	32
AISO1	132	2.06	0.83	biog	229	-13	30	43
AIMGA	120	1.34	1.07	biog	243	-11	28	39
AAVB1	198	-2.00	1.24	anth	313	-11	0	12
AAVB2	179	0.00	0.88	anth	271	-6	18	25
AMT6	168	3.00	0.15	biog	198	-3	41	43
ASVPO2	241	1.00	0.07	anth	249	-2	24	26
AMTHYD	186	1.72	0.30	biog	226	2	36	34
AMT1	300	-2.00	0.37	biog	299	5	19	14
AMT5	170	2.00	0.30	biog	213	8	44	37
AMT4	184	1.00	0.30	biog	224	20	49	29
ADIM	248	-3.16	0.72	biog	299	22	32	11
ASVPO1	230	0.00	0.12	anth	245	22	44	22
AMT3	186	0.00	0.44	biog	238	27	51	24
AIETET	136	-0.33	0.88	biog	238	30	55	25
AISO2	133	-0.21	0.85	biog	233	33	59	26
ASVOO3	134	2.00	0.35	anth	184	34	73	39
AMT2	200	-1.00	0.37	biog	243	42	62	20
ALVPO1	218	-1.00	0.18	anth	241	44	64	20
ASVOO2	135	1.00	0.45	anth	195	46	78	33
ASVOO1	135	0.00	0.57	anth	207	55	82	27
AORGC	177	-2.52	0.67	biog	251	58	73	15
ALVOO2	136	-1.00	0.71	anth	222	59	81	22
ALVOO1	136	-2.00	0.88	anth	238	60	77	17
AGLY	66.4	-1.34	0.77	biog	160	70	90	21
APCSO	170	-5.00	0.67	anth	245	96	108	12

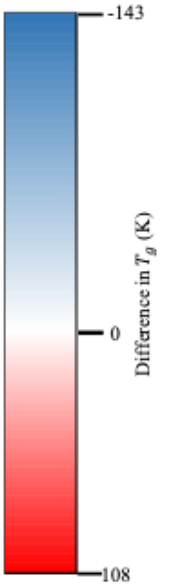

Line 390–394: I don't see why it is important to note that water diffusion from core to shell was not considered given the sensitivity of γIEPOX to kparticle. Please explain. Can you elaborate further on these sensitivity studies?

We thank the reviewer for the opportunity to further clarify the importance of this. Ultimately the amount of water in the inorganic aqueous core will alter both the pH and ion concentrations of this part of the aerosol – which is where IEPOX heterogeneous reactive uptake takes place. The more water in the inorganic aqueous core, the higher the pH, which will reduce the opening of the epoxydiol group, and also lower aqueous sulfate concentrations (the nucleophile responsible for attaching to the open carbo-cation after the epoxide group opens in the production of methyltetrol sulfates). In this same scenario, the formation of 2-methyltetrols will still be reduced

given the reduced epoxide opening step, however, there will be an abundance of water to attach to the free carbo-cation. Given that we do not account for the water equilibrium between the organic coating and the inorganic aqueous core, we are not able to capture this potential dilution impact.

We make the following changes to the methods section to explain the ring opening and nucleophilic attack processes:

Where $k_{particle}$ is the pseudo-first-order rate constant (s^{-1}) that takes into account the opening of the epoxydiol group on IEPOX by a proton (acid) followed by a nucleophilic attack (by sulfate, water, or monomer IEPOX-SOA species) on the free carbo-cation formed from this opening, and is represented by the following equation (Eddingsaas et al., 2010; Pye et al., 2013):

$$k_{particle} = \sum_{i=1}^{N} \sum_{j=1}^{M} k_{i,j}[nuc_i][acid_j] \quad (5)$$

Where $k_{i,j}$ are individual acid-nucleophile rate constants defined by Supplemental Table 3.

And elaborate on the significance of not accounting for organic-inorganic water equilibrium in the results:

With the implementation of phase separation, water equilibrium between ~~diffusing from the~~ the inorganic core and~~to~~ the organic coating was not considered. In reality water taken up by the organic shell could make it's way into the inorganic core given it's polar attraction, diluting both acidity and nucleophile concentrations, and therefore reducing $k_{particle}$. ~~and therefore inorganic ion aqueous concentrations were not directly impacted by phase separation.~~ This is important to note given γ_{IEPOX}'s sensitivity to $k_{particle}$. When~~that~~ increasing $k_{particle}$ from 10^{-3} s^{-1}~~/s~~ to 10^{-2} s^{-1}~~/s, results in an increase in~~ γ_{IEPOX} increases by ~740% of magnitude (assuming an organic coating radius of 50 nm and $T = 298K$) (SI Eq. 3). An increase in $D_{org,eff}$ from 10^{-13} m^2 s^{-1}~~/s~~ to 10^{-12} m^2 s^{-1}~~/s~~ results in an increase in γ_{IEPOX} by ~0.02% (assuming an organic coating radius of 50 nm and $T = 298K$) (SI Eq. 3). The impacts of internal water movement in phase separated aerosol requires further exploration, as it may be another important modulator of IEPOX heterogeneous reactive uptake, and other heterogeneous reactive uptake reactions.

Line 477: what is the rationale in increasing kparticle from 0.0001s−1 to 0.001s−1? Please elaborate. Additionally, also avoid using "/s" and use the standard unit "s−1" or "s−"

We thank the reviewer for following up on this point and hope that changes to our results section per the previous line comment have elaborated on this. We have also changed all units in-text and in figures and tables to use the -1 notation instead of /

Line 497: the atmospheric implication section is rather general and more suitable for introduction. Please tie the atmospheric implication to your results.

Thank you for your recommendation. We have revised this section to tie in our results with specific atmospheric implications including impacts on heterogeneous chemistry, impact on cloud droplet activation, cirrus cloud formation and trapping of hazardous air pollutants posed by inorganic-organic phase separation and viscous outer organic coatings.

Angell, C. A. Relaxation in liquids, polymers and plastic crystals — strong/fragile patterns and problems. *Journal of Non-Crystalline Solids, 131-133*, 13-31. doi:https://doi.org/10.1016/0022-3093(91)90266-9 (1991).

Armstrong, N. C., Chen, Y., Cui, T., Zhang, Y., Christensen, C., Zhang, Z., Turpin, B. J., Chan, M. N., Gold, A., Ault, A. P., & Surratt, J. D. Isoprene Epoxydiol-Derived Sulfated and Nonsulfated Oligomers Suppress Particulate Mass Loss during Oxidative Aging of Secondary Organic Aerosol. *Environmental Science & Technology, 56*(23), 16611-16620. doi:10.1021/acs.est.2c03200 (2022).

D'Ambro, E. L., Schobesberger, S., Gaston, C. J., Lopez-Hilfiker, F. D., Lee, B. H., Liu, J., Zelenyuk, A., Bell, D., Cappa, C. D., Helgestad, T., Li, Z., Guenther, A., Wang, J., Wise, M., Caylor, R., Surratt, J. D., Riedel, T., Hyttinen, N., Salo, V. T., Hasan, G., Kurtén, T., Shilling, J. E., & Thornton, J. A. Chamber-based insights into the factors controlling epoxydiol (IEPOX) secondary organic aerosol (SOA) yield, composition, and volatility. *Atmos. Chem. Phys., 19*(17), 11253-11265. doi:10.5194/acp-19-11253-2019 (2019).

DeRieux, W. S. W., Li, Y., Lin, P., Laskin, J., Laskin, A., Bertram, A. K., Nizkorodov, S. A., & Shiraiwa, M. Predicting the glass transition temperature and viscosity of secondary organic material using molecular composition. *Atmos. Chem. Phys., 18*(9), 6331-6351. doi:10.5194/acp-18-6331-2018 (2018).

Diveky, M. E., Gleichweit, M. J., Roy, S., & Signorell, R. Shining New Light on the Kinetics of Water Uptake by Organic Aerosol Particles. *The Journal of Physical Chemistry A, 125*(17), 3528-3548. doi:10.1021/acs.jpca.1c00202 (2021).

Gilliam, R. C., Hogrefe, C., & Rao, S. T. New methods for evaluating meteorological models used in air quality applications. *Atmospheric Environment, 40*(26), 5073-5086. doi:https://doi.org/10.1016/j.atmosenv.2006.01.023 (2006).

Hodas, N., Zuend, A., Mui, W., Flagan, R. C., & Seinfeld, J. H. Influence of particle-phase state on the hygroscopic behavior of mixed organic–inorganic aerosols. *Atmos. Chem. Phys., 15*(9), 5027-5045. doi:10.5194/acp-15-5027-2015 (2015).

Hu, W., Palm, B. B., Day, D. A., Campuzano-Jost, P., Krechmer, J. E., Peng, Z., de Sá, S. S., Martin, S. T., Alexander, M. L., Baumann, K., Hacker, L., Kiendler-Scharr, A., Koss, A. R., de Gouw, J. A., Goldstein, A. H., Seco, R., Sjostedt, S. J., Park, J. H., Guenther, A. B., Kim, S., Canonaco, F., Prévôt, A. S. H., Brune, W. H., & Jimenez, J. L. Volatility and lifetime against OH heterogeneous reaction of ambient isoprene-epoxydiols-derived secondary organic aerosol (IEPOX-SOA). *Atmos. Chem. Phys., 16*(18), 11563-11580. doi:10.5194/acp-16-11563-2016 (2016).

Jimenez, J. L., Canagaratna, M. R., Donahue, N. M., Prevot, A. S. H., Zhang, Q., Kroll, J. H., DeCarlo, P. F., Allan, J. D., Coe, H., Ng, N. L., Aiken, A. C., Docherty, K. S., Ulbrich, I. M.,

Grieshop, A. P., Robinson, A. L., Duplissy, J., Smith, J. D., Wilson, K. R., Lanz, V. A., Hueglin, C., Sun, Y. L., Tian, J., Laaksonen, A., Raatikainen, T., Rautiainen, J., Vaattovaara, P., Ehn, M., Kulmala, M., Tomlinson, J. M., Collins, D. R., Cubison, M. J., Dunlea, J., Huffman, J. A., Onasch, T. B., Alfarra, M. R., Williams, P. I., Bower, K., Kondo, Y., Schneider, J., Drewnick, F., Borrmann, S., Weimer, S., Demerjian, K., Salcedo, D., Cottrell, L., Griffin, R., Takami, A., Miyoshi, T., Hatakeyama, S., Shimono, A., Sun, J. Y., Zhang, Y. M., Dzepina, K., Kimmel, J. R., Sueper, D., Jayne, J. T., Herndon, S. C., Trimborn, A. M., Williams, L. R., Wood, E. C., Middlebrook, A. M., Kolb, C. E., Baltensperger, U., & Worsnop, D. R. Evolution of Organic Aerosols in the Atmosphere. *Science, 326*(5959), 1525-1529. doi:10.1126/science.1180353 (2009).

Lambe, A. T., Onasch, T. B., Massoli, P., Croasdale, D. R., Wright, J. P., Ahern, A. T., Williams, L. R., Worsnop, D. R., Brune, W. H., & Davidovits, P. Laboratory studies of the chemical composition and cloud condensation nuclei (CCN) activity of secondary organic aerosol (SOA) and oxidized primary organic aerosol (OPOA). *Atmos. Chem. Phys., 11*(17), 8913-8928. doi:10.5194/acp-11-8913-2011 (2011).

Li, W., Teng, X., Chen, X., Liu, L., Xu, L., Zhang, J., Wang, Y., Zhang, Y., & Shi, Z. Organic Coating Reduces Hygroscopic Growth of Phase-Separated Aerosol Particles. *Environmental Science & Technology, 55*(24), 16339-16346. doi:10.1021/acs.est.1c05901 (2021).

Lienhard, D. M., Huisman, A. J., Krieger, U. K., Rudich, Y., Marcolli, C., Luo, B. P., Bones, D. L., Reid, J. P., Lambe, A. T., Canagaratna, M. R., Davidovits, P., Onasch, T. B., Worsnop, D. R., Steimer, S. S., Koop, T., & Peter, T. Viscous organic aerosol particles in the upper troposphere: diffusivity-controlled water uptake and ice nucleation? *Atmos. Chem. Phys., 15*(23), 13599-13613. doi:10.5194/acp-15-13599-2015 (2015).

Maskey, S., Chong, K. Y., Kim, G., Kim, J.-S., Ali, A., & Park, K. Effect of mixing structure on the hygroscopic behavior of ultrafine ammonium sulfate particles mixed with succinic acid and levoglucosan. *Particuology, 13*, 27-34. doi:https://doi.org/10.1016/j.partic.2013.08.004 (2014).

Massoli, P., Lambe, A. T., Ahern, A. T., Williams, L. R., Ehn, M., Mikkilä, J., Canagaratna, M. R., Brune, W. H., Onasch, T. B., Jayne, J. T., Petäjä, T., Kulmala, M., Laaksonen, A., Kolb, C. E., Davidovits, P., & Worsnop, D. R. Relationship between aerosol oxidation level and hygroscopic properties of laboratory generated secondary organic aerosol (SOA) particles. *Geophysical Research Letters, 37*(24). doi:https://doi.org/10.1029/2010GL045258 (2010).

Pajunoja, A., Lambe, A. T., Hakala, J., Rastak, N., Cummings, M. J., Brogan, J. F., Hao, L., Paramonov, M., Hong, J., Prisle, N. L., Malila, J., Romakkaniemi, S., Lehtinen, K. E. J., Laaksonen, A., Kulmala, M., Massoli, P., Onasch, T. B., Donahue, N. M., Riipinen, I., Davidovits, P., Worsnop, D. R., Petäjä, T., & Virtanen, A. Adsorptive uptake of water by semisolid secondary organic aerosols. *Geophysical Research Letters, 42*(8), 3063-3068. doi:https://doi.org/10.1002/2015GL063142 (2015).

Parsons, M. T., Mak, J., Lipetz, S. R., & Bertram, A. K. Deliquescence of malonic, succinic, glutaric, and adipic acid particles. *Journal of Geophysical Research: Atmospheres, 109*(D6). doi:https://doi.org/10.1029/2003JD004075 (2004).

Pleim, J. E., & Gilliam, R. An Indirect Data Assimilation Scheme for Deep Soil Temperature in the Pleim–Xiu Land Surface Model. *Journal of Applied Meteorology and Climatology, 48*(7), 1362-1376. doi:https://doi.org/10.1175/2009JAMC2053.1 (2009).

Pleim, J. E., & Xiu, A. Development of a Land Surface Model. Part II: Data Assimilation. *Journal of Applied Meteorology, 42*(12), 1811-1822. doi:https://doi.org/10.1175/1520-0450(2003)042<1811:DOALSM>2.0.CO;2 (2003).

Pye, H. O. T., Murphy, B. N., Xu, L., Ng, N. L., Carlton, A. G., Guo, H., Weber, R., Vasilakos, P., Appel, K. W., Budisulistiorini, S. H., Surratt, J. D., Nenes, A., Hu, W., Jimenez, J. L., Isaacman-VanWertz, G., Misztal, P. K., & Goldstein, A. H. On the implications of aerosol liquid water and phase separation for organic aerosol mass. *Atmos. Chem. Phys., 17*(1), 343-369. doi:10.5194/acp-17-343-2017 (2017).

Riedel, T. P., Lin, Y.-H., Budisulistiorini, S. H., Gaston, C. J., Thornton, J. A., Zhang, Z., Vizuete, W., Gold, A., & Surratt, J. D. Heterogeneous Reactions of Isoprene-Derived Epoxides: Reaction Probabilities and Molar Secondary Organic Aerosol Yield Estimates. *Environmental Science & Technology Letters, 2*(2), 38-42. doi:10.1021/ez500406f (2015).

Riedel, T. P., Lin, Y. H., Zhang, Z., Chu, K., Thornton, J. A., Vizuete, W., Gold, A., & Surratt, J. D. Constraining condensed-phase formation kinetics of secondary organic aerosol components from isoprene epoxydiols. *Atmos. Chem. Phys., 16*(3), 1245-1254. doi:10.5194/acp-16-1245-2016 (2016).

Schmedding, R., Rasool, Q. Z., Zhang, Y., Pye, H. O. T., Zhang, H., Chen, Y., Surratt, J. D., Lopez-Hilfiker, F. D., Thornton, J. A., Goldstein, A. H., & Vizuete, W. Predicting secondary organic aerosol phase state and viscosity and its effect on multiphase chemistry in a regional-scale air quality model. *Atmos. Chem. Phys., 20*(13), 8201-8225. doi:10.5194/acp-20-8201-2020 (2020).

Su, Q., Wong, D. C., Wang, Y., Zhang, K., Skipper, T. N., Farrell, S. L., Huang, L., Chen, Y., Yi, Y., Tan, J., Pye, H. O. T., & Li, L. Enhanced Isoprene Secondary Organic Aerosol Formation with C5-alkene Triols Newly Added to Current Chemical Mechanisms. *ACS ES&T Air, 2*(9), 1939-1950. doi:10.1021/acsestair.5c00124 (2025).

Tan, F., Zhang, H., Xia, K., Jing, B., Li, X., Tong, S., & Ge, M. Hygroscopic behavior and aerosol chemistry of atmospheric particles containing organic acids and inorganic salts. *npj Climate and Atmospheric Science, 7*(1), 203. doi:10.1038/s41612-024-00752-9 (2024).

Yan, J., Armstrong, N. C., Kolozsvari, K. R., Waters, C. M., Xiao, Y., Fankhauser, A. M., Cooke, M. E., Frauenheim, M., Buchenau, N. A., Parham, R. L., Zhang, Z., Turpin, B. J., Lambe, A. T., Gold, A., Ault, A. P., & Surratt, J. D. Effect of Initial Seed Aerosol Acidity on the Kinetics and Products of Heterogeneous Hydroxyl Radical Oxidation of Isoprene Epoxydiol-Derived Secondary Organic Aerosol. *The Journal of Physical Chemistry A, 129*(18), 4132-4147. doi:10.1021/acs.jpca.4c08082 (2025).

Yan, J., Zhang, Y., Chen, Y., Armstrong, N. C., Buchenau, N. A., Lei, Z., Xiao, Y., Zhang, Z., Lambe, A. T., Chan, M. N., Turpin, B. J., Gold, A., Ault, A. P., & Surratt, J. D. Kinetics and Products of Heterogeneous Hydroxyl Radical Oxidation of Isoprene Epoxydiol-Derived Secondary Organic Aerosol. *ACS Earth and Space Chemistry, 7*(10), 1916-1928. doi:10.1021/acsearthspacechem.3c00073 (2023).